Archives of Dermatological Research (2019) 311:193–201
https://doi.org/10.1007/s00403-019-01901-4

ORIGINAL PAPER

Activators of SIRT1 in wound repair: an animal model study

Ana Cristina Christovam[1] · Viviane Theodoro[1] · Fernanda Aparecida Sampaio Mendonça[1] · Marcelo Augusto Marretto Esquisatto[1] · Gláucia Maria Tech dos Santos[1] · Maria Esméria Corezola do Amaral[1]

Received: 27 November 2018 / Revised: 13 February 2019 / Accepted: 15 February 2019 / Published online: 19 February 2019

Abstract
Caloric restriction (CR) and resveratrol activate SIRT1 and induce anti-inflammatory and antioxidant properties. We perform excisional lesion on the dorsum of four groups anesthetized animals: ad libitum-AL diet, AL diet with topical application of 2% resveratrol-Rv, 30% calorie restricted, and finally 30% calorie restricted with 2% resveratrol and we examine CR and Rv effects in wound repair. Restricted animals remained with CR for 31 days. The lesion was performed on day 18 of CR, and resveratrol application was started on day 19. Lesion samples were then collected on days 3 and 10 of treatment for structural, morphometric, and protein analyses. Our results showed that CR and Rv group as well as R group had enhanced numbers of blood vessels, VEGF, fibroblast, birefringent collagen fiber areas in the lesion. We conclude that effects in wound repair suggests that both CR and resveratrol may modulate angiogenesis, fibroplasia, and collagenesis, which could be ascribed to the action of SIRT1.

Keywords Resveratrol · Caloric restriction · Tissue repair · SIRT1 · Skin · Collagen

Introduction

The reestablishment of tissue integrity after lesion involves coordinated processes that include inflammatory responses, formation of granulation tissue, cell proliferation, and remodeling of the final tissue [11]. Factors that can hinder the healing process include obesity, diabetes mellitus, and malnutrition. A satisfactory nutritional status, which is directly dependent on the diet, is essential for successful wound repair [19]. Cell migration, angiogenesis, collagen deposition, granulation tissue formation, and tissue remodeling are repair processes that are intrinsically linked to the availability of energy substrates, proteins, and micronutrients [43]. Adequate amounts of carbohydrates, fats, and proteins are required for healing to occur, while experimental evidence suggests that specific nutritional interventions can have significant beneficial effects in wound repair [18, 40].

There is debate in the literature concerning the effects of caloric restriction (CR) on wound repair. Earlier studies showed that CR retarded healing in rodents [12, 32]. Retardation has also been found for collagen production [38] and the healing of skin tissue [14] in calorie-restricted animals. In contrast, a study conducted to evaluate the effects of age and CR on the healing process in rats and monkeys found that the rates of healing were similar for CR groups and control animals fed ad libitum [34]. Reed et al. [31] showed that over the long term, CR assisted in preserving proliferative capacity and increasing the capacity to synthesize structural proteins and trophic factors required for wound repair.

CR leads to the activation of sirtuin proteins [7] related to the regulation of collagen transcription and inflammation [45]. Seven members of the sirtuin family are involved in many cellular processes [7]. SIRT1 appears to be involved in fibrotic diseases and regulation of TGF-β1 during mesenchymal–epithelial transition, as well as cell proliferation, differentiation, and survival [36, 45].

The metabolic and hormonal alterations induced by CR have led to the identification of synthetic and natural compounds able to reproduce its effects. One of these compounds is resveratrol [3, 28, 37], which is a polyphenol found in grape seeds and red wines. Wine polyphenols are known for their capacity to mimic the effect of CR in

✉ Maria Esméria Corezola do Amaral
esmeria@uniararas.br

[1] Graduate Program in Biomedical Sciences, Centro Universitário da Fundação Hermínio Ometto, FHO, Av. Maximiliano Barutto 500, Jardim Universitário, Araras, SP 13607-339, Brazil

activation of SIRT1 [9, 13]. A formulation of resveratrol in nanospheres, used as a cosmeceutical, has been suggested to have rejuvenation properties, due mainly to its antioxidant activity [5, 48]. Resveratrol has also been reported to act as a photoprotective agent against skin cancer [24]. Various effects of resveratrol have been found in angiogenesis [8] and the healing of incisional wounds [46], cartilage [22], and bone defects [6]. However, uncertainty remains concerning the effect of resveratrol in the healing of cutaneous wounds. An advantage of using resveratrol in local topical applications to the skin is that it avoids systemic side effects. Therefore, the aim of this study was to evaluate the effects of CR and resveratrol, as activators of SIRT1, in the healing of excisional skin wounds on the dorsum of rats.

Materials and methods

Animals

Thirty-two male Wistar rats (*Rattus norvegicus albinus*) aged approximately 120 days and with average weight of around 350 g were obtained from the Animal Experimentation Center of UNIARARAS. The animals were housed in individual cages, at constant temperature (23 ± 2 °C) and humidity (55%), with a 12:12 h light/dark cycle. During an initial period of five days, to adapt to social isolation, the animals received food and water ad libitum. The feed was weighed daily to determine the average food consumption of the animals.

Experimental groups

The animals were randomly divided into four groups of eight individuals, as follows: AL: ad libitum diet and topical application of the vehicle, without resveratrol produced using 50 mg of DMSO (dimethyl sulfoxide), 0.096 g of Microcel MC-101 (microcrystalline cellulose), 0.004 g of Aerosil, and 10 g of Pentravan qsp; ALRv: ad libitum diet and topical application of the formulation with 2% resveratrol (Sigma, Stockholm, Sweden) [29]; R: 30% CR and topical application of the vehicle; RRv: 30% CR and topical application of 2% resveratrol.

Caloric restriction

The control group continued with the same commercial feed (Nuvilab®—Nestlé Purina—Brazil) ad libitum, while the 30% CR group received 70% of the caloric intake of the control group [39], characterizing moderate CR. Calculation of the amount of feed provided was performed daily, by weighing the amount offered and the amount remaining in the case of the control animals, hence determining the amount ingested for the control group and enabling calculation of the 70% feed value for the restricted group. This procedure was performed during the 31 days of the experiment. Body weight was measured once weekly throughout the experiment.

Surgical procedure

The skin lesion operations were performed after 18 days of CR, following anesthetization of the animals with a mixture of ketamine hydrochloride (100 mg/kg) and xylazine hydrochloride (10 mg/kg) were purchased from Cristália (Itapira, SP, BR), administered intraperitoneally. After trichotomy on the skin of the dorsum, using a scalpel and a 10 mm^2 guide, excision was made of a cutaneous fragment consisting of the epidermis and the dermis, such that the dorsal muscle fascia was exposed. After creation of the lesions, the animals were returned to individual cages and were administered an analgesic with sodium dipyrone (10 mg/kg) was used in the water supplied to the animals for 72 h.

The specific treatments of the groups were started 24 h after the surgery (on day 19) and were performed daily at the same time during 10 days. Samples were collected for histomorphometric, biochemical, and molecular analyses on days 3 and 10 after the surgery. Blood glucose was determined using reagent strips and a glucose meter (Abbott, Chicago, USA), on the day of euthanasia, with the animals having been fasted for 6 h.

Chemicals and reagents

The chemicals for topical application were resveratrol and DMSO (dimethyl sulfoxide) were purchased from Sigma-Aldrich (St. Louis, MO, USA), Microcel MC-101 (microcrystalline cellulose) from Blanver Farmoquimica (São Paulo, SP, BR), Aerosil from Evonik Brazil Ltda (São Paulo, SP, BR), Pentravan from Fragon (Rotterdam, Netherlands). The dyes for tissue structural and morphometric analysis Formaldehyde, Picrosirius–hematoxylin, Toluidine Blue, Mallory's trichrome (it uses the three stains: aniline blue, acid fuchsin, and orange G) were obtained from Sigma-Aldrich and Paraplast (Histosec) was purchased from Merck (Kenilworth, NJ, USA). The chemicals for Western Blotting were tris-[hydroxymethyl]aminomethane (Tris), phenylmethylsulfonyl fluoride (PMSF), dithiothreitol (DTT), Triton X-100, Tween 20, and glycerol were purchased from Sigma-Aldrich. The reagents and apparatus for sodium dodecyl sulfate-polyacrylamide gel electrophoresis (SDS-PAGE) and immunoblotting were from Bio-Rad (Richmond, CA, USA). Aprotinin was purchased from Bayer (São Paulo, SP, Brazil). PVDF transfers membranes 0.45 µm pore sizes was obtained from Bio Rad® (Hercules, CA, USA), ECL Chemiluminescence

from Thermo Fisher Scientific (Waltham, MA USA). TGF-β1, VEGF and FGF antibodies were obtained Santa Cruz Biotechnology (Dallas, Texas, USA), SIRT1 antibody from Cell Signaling (Billerica, MA, USA) and anti-collagens I and III from Sigma-Aldrich. Anti-mouse, anti-rabbit, and anti-goat IgG1:HRP antibodies were purchased from Santa Cruz Biotechnology.

Collection and preparation of tissue for structural and morphometric analysis

Samples were removed from four animals of each group on days 3 and 10 after performing the lesions. An area of 25 mm^2 was delimited in the center of the lesion, to obtain standardized samples. The tissue fragments were immersed for 24 h in fixing solution consisting of 10% formaldehyde in Millonig buffer (pH 7.4), at ambient temperature. The pieces were then washed in buffer and embedded in Paraplast (Histosec, Merck), according to the standard procedure.

Longitudinal sections of the pieces, with thickness of 6 µm, were used for the different analyses. Picrosirius–hematoxylin staining and standard optical microscopy was used to observe the organization of the collagen fibers. Mallory's trichrome staining was used to quantify the content of collagen fibers in the repair area (% of total area). Toluidine Blue in McIlvaine buffer (pH 4.0) was used for structural analysis of the epidermis and dermis, together with determination of the numbers of fibroblasts and blood vessels. Dominici's stain was used for the quantification of inflammatory infiltrate. Evaluation of the organization and maturation of collagen fibers was performed by quantifying the birefringent fiber area, relative to the total fiber area, employing the picrosirius–hematoxylin method under polarized light [33]. Mallory's trichrome staining enabled separation of the fields according to the color distribution. The color range was defined at the beginning of the analysis and was the same for all the images quantified. The color band was adjusted until the areas representative of collagen became separated in the image. The same range was used to identify the collagen fibers in all the digitized fields. The area occupied was then calculated for each field. A Leica DM2000 photomicroscope was used to capture and digitize images of the sections removed from the central regions of the lesions.

The digitized images for four animals from each group were used to obtain five areas of 10^4 μm^2 for each central lesion section obtained on days 3 and 10 of treatment. These were analyzed using the Leica image measurement virtual grid and SigmaScan Pro 6.0™ software to determine the following morphometric parameters: total number of fibroblasts and inflammatory infiltrate ($n/10^4$ μm^2), number of neoformed blood vessels ($n/10^4$ μm^2), and percentage of birefringent collagen fibers in the healing area (%).

Western blotting

The lesion sections were homogenized for 30 s in protein extraction buffer (10 mM EDTA, 100 mM Trizma base, 10 mM sodium pyrophosphate, 100 mM sodium fluoride, 100 mM sodium orthovanadate, 2 mM PMSF, 0.1 mg/mL aprotinin, and distilled water). The extract was centrifuged for 45 min at 1500 rpm and 4 °C to remove the insoluble material. The supernatant was collected for the determination of the total protein concentration of the samples by the Biureto method (Protal colorimetric method, Laborlab, São Paulo, Brazil). Samples containing 30 µg protein were treated with Laemmli buffer containing 10 mM DDT and were used for SDS-PAGE with 10–12% tris-acrylamide in a minigel apparatus (Miniprotean). After the SDS-PAGE run, the proteins were transferred to PVDF membranes (Bio-Rad) and incubated for 2 h in blocking solution to reduce nonspecific protein binding. The membranes were then incubated for 4 h with specific antibodies for the proteins anti-TGF-β1, anti-VEGF, and anti-FGF (diluted 1:200), anti-SIRT1 (diluted 1:1000) and anti-collagens I and III (diluted 1:1000). Next, the membranes were incubated with specific anti-mouse, anti-rabbit, and anti-goat IgG1:HRP antibodies (diluted 1:10,000). Finally, the membranes were photodocumented using a SynGene G:BOX (Frederick, Maryland, USA) apparatus. The intensities of the bands were evaluated by densitometry [25].

Measurement of TBARS (thiobarbituric acid-reactive substances) and total sulfhydryl content

TBARS were determined as described by Ohkawa et al. [26]. Measurement was principally made of malondialdehyde (MDA), a product of lipoperoxidation caused mainly by hydroxyl free radicals. The TBARS concentration was determined spectrophotometrically at 532 nm and was expressed as nmol of MDA per mg of protein.

The measurement of sulfhydryl groups was based on the method of [1]. The reduction of DTNB (5,5-dithio-bis(2-nitrobenzoic acid)) by thiols produces a yellow derivative that can be determined spectrophotometrically using its absorbance at 412 nm. The sulfhydryl content is inversely correlated with the oxidative damage to proteins. The results were calculated as nmol of TNB per mg of protein.

Analysis of the results

Comparative analysis of the data for the different groups was performed using ANOVA followed by the Bonferroni test, comparing the treatment groups (ALRv, R, and RRv) with the AL group. The results were expressed as mean ± standard error of the mean ($X \pm$ SEM), and the level of significance adopted was 5% ($p < 0.05$).

Results

Body weight, food intake, and glycemia of the animals

Figure 1 shows the establishment of the CR animal model from the analyses of body weight, food intake, and glycemia. The animals of groups R and RRv lost weight, compared to groups AL and ALRv ($p=0.003$) (Fig. 1a). The food intakes of the animals in groups R and RRv were lower on days 7, 14, 21, and 31 of the experiment, compared to the animals of groups AL and ALRv (Fig. 1b, $p=0.04$). On days 3 and 10 of treatment, the glycemia values of animals in groups R and RRv were significantly lower than those of the AL and ALRv animals (Fig. 1c, $p=0.03$).

Structural analyses of the skin lesion area

The morphological characteristics of the repair tissue were compared for the different groups over the experimental period. The data were obtained from the qualitative and quantitative analyses of the biological features during the inflammatory phase on day 3 (leucocyte infiltration, hemorrhage, and exudate) and the proliferative phase on day 10 (fibroblastic hyperplasia, re-epithelialization, and angiogenesis).

On day 3, fibroblasts were present in large quantities at the edges of the lesion, between the repair area and the original preserved tissue. Keratinocytes showed greater proliferation on day 10, while the presence of blood vessels gradually increased during the experimental period, especially in the central part of the repair area. Figure 2 shows the distribution and organization of the collagen fibers. On day 3, thin fibers were distributed parallel to the longer axis of the repair area, close to the blood vessels and near the surface of the lesion. On day 10, thicker fibers were distributed throughout the dermis, oriented perpendicular to the longer axis of the lesion.

Morphometric analysis of the lesion area

Analysis of the morphometric variables revealed several quantitative differences between the groups during the experimental period (Table 1). No significant differences were observed for the inflammatory infiltrate in samples taken from the different groups and at different times. Compared to the AL group, the numbers of blood vessels were higher for the RRv group on days 3 ($p=0.03$) and 10 ($p=0.04$), and for the R group only on day 10 ($p=0.04$). No differences in fibroblast numbers were observed between the groups on day 3. However, an increase was found for the RRv group on day 10 ($p=0.04$). The area percentages of collagen fibers were similar for all the groups and experimental periods. However, the area of birefringent collagen fibers was higher for the RRv group, compared to the other groups, on days 3 ($p=0.04$) and 10 ($p=0.04$).

Western blotting protein analysis of the lesion area

On day 3, increased expression of collagen I was observed for groups R and RRv, compared to groups AL and ALRv ($p=0.01$). On day 10, groups ALRv, R, and RRv showed higher expression of collagen I, compared to the AL group

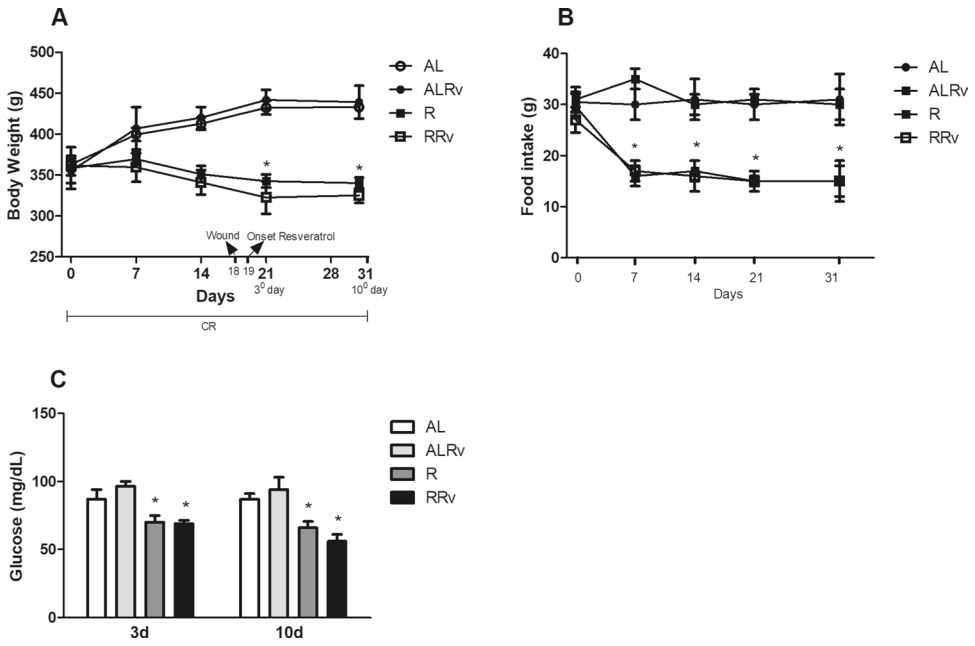

Fig. 1 Effects of resveratrol and CR on **a** weight gain, **b** food intake, and **c** glycemia of the animals in groups AL, ALRv, R, and RRv during the experimental period. Data are shown as means ± standard errors ($n=4$). *$p<0.05$ for AL and ALRv vs. R and RRv

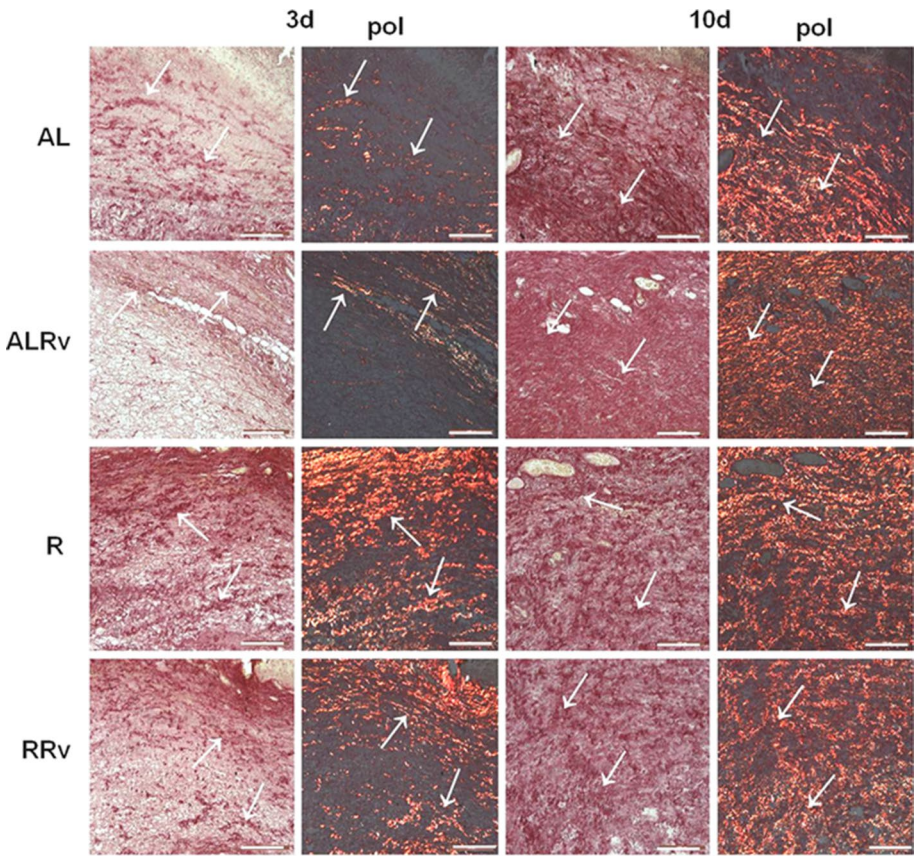

Fig. 2 Representative photomicrographs of birefringent collagen fibers in the transverse sections of samples from the lesion areas of animals in the AL, ALRv, R, and RRv groups on days 3 and 10 of treatment. The sections were stained with picrosirius–hematoxylin and were analyzed under clear field and polarized (pol) light. The arrow indicates collagen fibers. Bar: 100 µm

(Fig. 3; $p=0.03$). Higher collagen III was found for the ALRv, R, and RRv groups, compared to the AL group, on days 3 ($p=0.03$) and 10 ($p=0.01$). On day 10, VEGF protein expression was higher for groups R and RRv, compared to groups AL and ALRv ($p=0.03$). The values obtained for the FGF and TGF-β1 proteins were similar for all groups and times, while SIRT1 was higher for the ALRv and R groups, compared to the AL group, on days 3 and 10.

Analysis of the product of oxidative stress and alteration of antioxidant capacity

On day 3, the concentration of TBARS was significantly lower for the groups that received resveratrol treatment (ALRv and RRv), compared to groups AL and R ($p=0.01$) (Fig. 4). On day 10, there was no difference between the groups. TBARS originates from the reaction of low molecular weight aldehydes, especially malondialdehyde, with thiobarbituric acid. These aldehydes are derived from lipid peroxidation of the unsaturated fatty acids of biological membranes [23, 27].

On day 3, the concentration of reduced thiols (–SH groups) was higher for groups ALRv and RRv, compared to the resveratrol treatment groups AL and R ($p=0.01$). On day 10, there was only a significant difference in comparing group ALRv with groups AL, R, and RRv ($p=0.01$). Reduced thiol groups are mainly present in reduced glutathione and the cysteine residues of proteins. These groups are preferential targets of reactive species, and therefore, act as antioxidants, with decreases in their concentrations being associated with a state of oxidative stress [44].

Discussion

During the repair process, fibroblasts are activated and become transformed to myofibroblasts that migrate to the area of the lesion, where they assist in closing the wound by promoting the synthesis and secretion of collagen [20]. Reed et al. [31] reported that calorie-restricted mice showed greater capacity for wound repair, compared to mice fed ad libitum, with the effect appearing to be mediated, in part, by the increase of proliferative cells and collagen biosynthesis. In older Rhesus monkeys, 30% CR performed for 7 years led to beneficial effects by reducing collagen glycation [35]. Here, increases of type I collagen were observed on days 3 and 10, leading to reorganization of collagen in groups ALRv, R, and RRv [46] found that resveratrol increased fibroblast maturation and collagen deposition *in vivo*. In the present study, the increase in collagen I could have been related to a possible participation of SIRT1, since the data showed that on day 3 this protein was present at

Table 1 Morphometric parameters evaluated for samples from the repair area for groups AL, ALRv, R, and RRv on days 3 and 10 of treatment

Times		Day 3	Day 10
Parameters	Groups		
Inflammatory infiltrate ($n/10^4$ μm^2)	AL	20.3 ± 3.1	13.9 ± 3.1
	ALRv	19.9 ± 2.3	14.4 ± 2.7
	R	18.2 ± 3.9	13.5 ± 2.3
	RRv	22.3 ± 2.6	14.5 ± 2.2
Blood vessels ($n/10^4$ μm^2)	AL	1.3 ± 0.3	1.7 ± 0.4
	ALRv	1.2 ± 0.3	1.8 ± 0.3
	R	1.9 ± 0.2	2.4 ± 0.4*
	RRv	2.1 ± 0.4*	2.5 ± 0.2*
Collagen fiber content (% of area)	AL	26,7 ± 4,1	44.2 ± 5.3
	AL	26.7 ± 4.1	44.2 ± 5.3
	ALRv	28.5 ± 4.9	47.2 ± 5.7
	R	30.1 ± 3.9	49.7 ± 4.1
	RRv	33.2 ± 4.2	52.4 ± 3.9
Birefringent collagen fibers (% of area)	AL	13.8 ± 2.5	38.7 ± 6.3
	ALRv	14.5 ± 3.3	39.2 ± 5.2
	R	34.1 ± 4.2*	52.7 ± 4.9*
	RRv	39.1 ± 5.6*	54.8 ± 5.1*
Fibroblasts ($n/10^4$ μm^2)	AL	22.3 ± 4.5	32.9 ± 3.8
	ALRv	23.8 ± 3.9	39.1 ± 2.7
	R	24.2 ± 2.6	34.2 ± 4.3
	RRv	25.1 ± 3.1	45.2 ± 3.1*

The values are presented as the means and standard errors for each group ($n = 4$)

*$p < 0.05$ vs. group AL

higher levels in the same groups. Decreased SIRT1 on day 10 was indicative of adaptation of the tissue to the diet and resveratrol. The basis for this conclusion was that SIRT1 exhibits antioxidative, angiogenic, anti-inflammatory, and anti-apoptotic properties [30], which are essential in activation of the initial responses to CR and to damaged tissue. In contrast, it has also been reported that resveratrol reduces fibroblast proliferation, hydroxyproline, and expression of collagens I and III in hypertrophic lesions [2, 47]. This was in contrast to the findings of [46], who found that administration of resveratrol by gavage in females acted to increase fibroblasts and collagen deposition, in agreement with the present results concerning the use of resveratrol. In another study, it was shown that resveratrol suppressed proliferation and induced apoptosis in keloid fibroblasts, but did not decrease either type I collagen or the proliferation of normal skin fibroblasts [15].

Bashmakov et al. [4] attributed the upregulation of TGF-β1 in diabetic foot wounds to an anti-inflammatory effect of resveratrol. In the experimental model used here, the same effect was observed for the RRv group on day 10, relative to day 3, since a reduction of this proinflammatory factor was observed, suggesting a relation with the decrease of SIRT1 for the same period and animal group.

It has been shown that resveratrol induces VEGF expression and, consequently, acts to regulate angiogenesis [46]. This regulation was also observed here and was probably associated with the expression of SIRT1, since VEGF is an activator of the latter. VEGF and bFGF are growth factors that also present pro-angiogenic properties, with both being essential for healing. In addition to being angiogenic, bFGF influences the proliferation of endothelial cells and fibroblasts [10].

The correct balance between oxidative attack and antioxidant capacity regulates the activity of most of the proteins present in the cells [21]. For example, the SIRT1 protein is activated by the reduction (oxidation–reduction reaction) of thiol groups present in its structure, promoted by the APE1/Ref-1 redox factor. This is of great importance for the homeostasis of endothelial tissue, mainly due to increased production of NO., which modulates tissue relaxation [17]. Other important activities in the processes of tissue repair and inflammation have also been attributed to this redox factor [41, 42], such as DNA repair and regulation of transcription factors related to cell survival, apoptosis, and proliferation [42]. Here, the increased levels of thiols observed in the ALRv and RRv groups revealed the participation of SIRT1, indicating positive modulation of inflammation, angiogenesis, and collagenesis. The findings of this work showed that both CR and resveratrol, as activators of SIRT1, could positively modulate the repair of tissue wounds, due to the induction of angiogenesis, fibroplasia, and collagen organization.

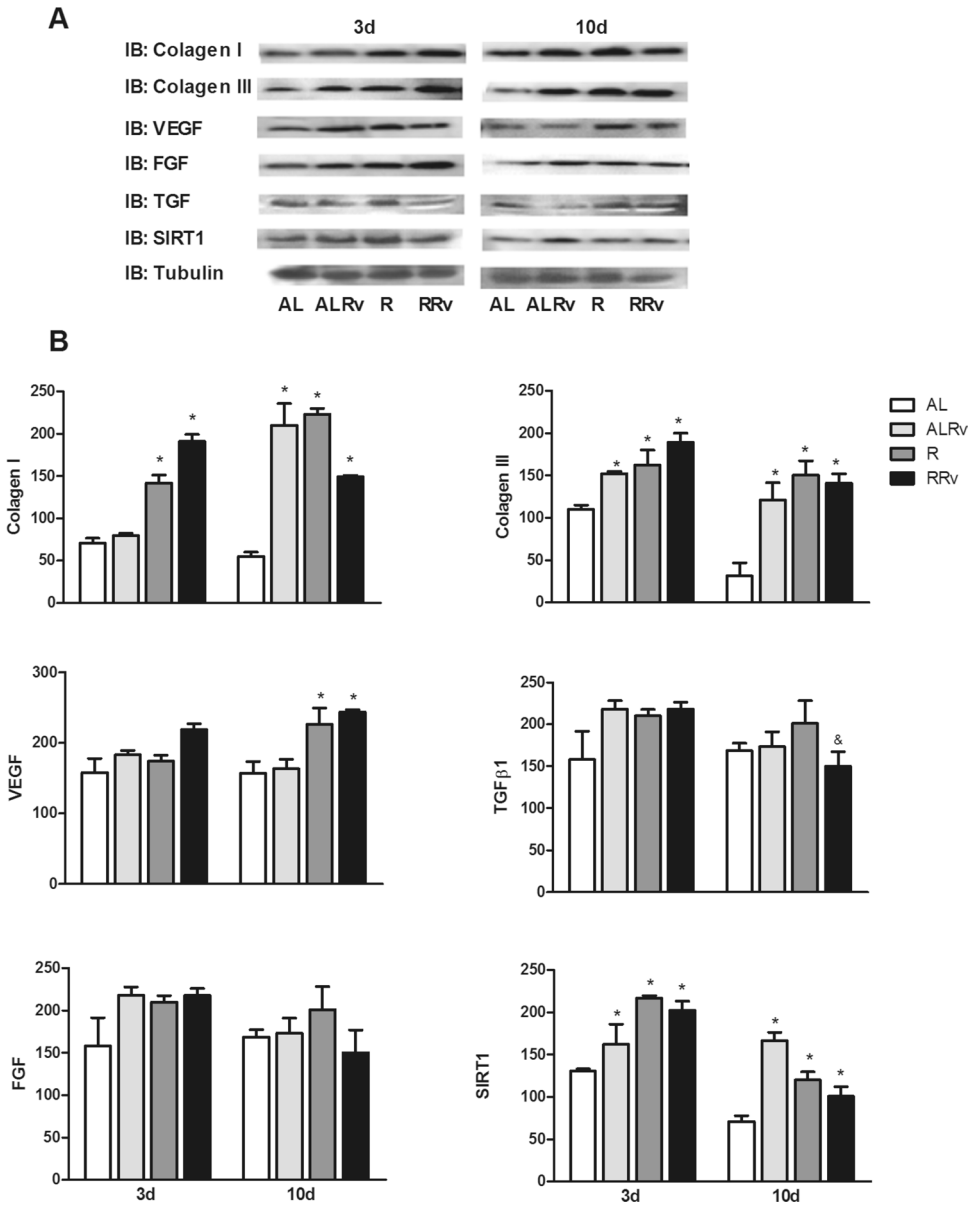

Fig. 3 Analysis of protein expression in the lesion samples for the AL, ALRv, R, and RRv animals: **a** representative bands of the proteins studied; **b** quantification of protein expression. The data are shown as means ± standard errors (n = 4). *$p < 0.05$ for the treatment groups vs. AL, and $p < 0.05$ for RRv (day 3) vs. RRv (day 10)

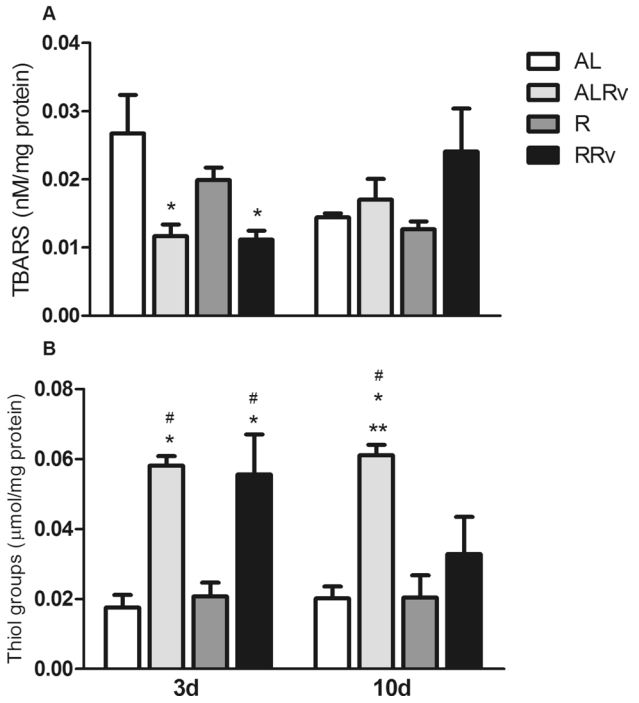

Fig. 4 Effects of resveratrol and CR on the TBARS (thiobarbituric acid-reactive substances) marker for oxidative stress and the marker for antioxidant activity (thiol groups), for the lesion samples from the different experimental groups. $^{*}p<0.05$ for AL vs. ALRv and RRv; $^{**}p<0.05$ for ALRv vs. RRv; $^{\#}p<0.05$ for R vs. ALRv and RRv ($n=4$)

Acknowledgements The authors are grateful to the students Amanda Tomazella, Bruna Assunção Bechtold, Leandro de Souza Rodrigues, and Rafaela Bresciani Rossi, who were responsible for the care of the animals and the collection of tissues on the day of euthanasia.

Funding This work was supported by the PROPesq-Uniararas (Pesquisa Institucional Uniararas).

Compliance with ethical standards

Conflict of interest The authors declare that there are no conflicts of interest.

Ethical approval All the surgical and experimental procedures employed in this study were performed according to the norms established by the Brazilian College of Animal Experimentation (COBEA) and were approved by the Animal Use Ethics Committee (CEUA) of UNIARARAS (protocol number 023/2014) and conducted according with the Guide for the Care and Use of Laboratory Animals [16].

References

1. Aksenov MY, Markesbery WR (2001) Changes in thiol content and expression of glutathione redox system genes in the hippocampus and cerebellum in Alzheimer's disease. Neurosci Lett 302:141–145
2. Bai XZ, Liu JQ, Yang LL et al (2016) Identification of sirtuin 1 as a promising therapeutic target for hypertrophic scars. Br J Pharmacol 173:1589–1601
3. Barger JL, Kayo T, Vann JM et al (2008) A low dose of dietary resveratrol partially mimics caloric restriction and retards aging parameters in mice. PLoS One 3(6):e2264
4. Bashmakov YK, Assaad-Khalil S, Petyaev IM (2011) Resveratrol may be beneficial in treatment of diabetic foot syndrome. Med Hypotheses 77:364–367
5. Baxter RA (2008) Anti-aging properties of resveratrol: review and report of a potent new antioxidant skin care formulation. J Cosmet Dermatol 7:2–7
6. Casarin RC, Casati MZ, Pimentel SP (2014) Resveratrol improves bone repair by modulation of bone morphogenetic proteins and osteopontin gene expression in rats. Int J Oral Maxillofac Surg 43:900–906
7. Chang HC, Guarente L (2014) SIRT1 and other sirtuins in metabolism. Trends Endocrinol Metab 25:138–145
8. Chen Y, Tseng S-H (2007) Pro- and anti-angiogenesis effects of resveratrol. Vivo 21:365–370
9. Chung JH, Manganiello V, Dyck JR (2012) Resveratrol as a calorie restriction mimetic: therapeutic implications. Trends Cell Biol 22:546–554
10. Feito MJ, Lozano RM, Alcaide M (2011) Immobilization and bioactivity evaluation of FGF-1 and FGF-2 on powdered silicon-doped hydroxyapatite and their scaffolds for bone tissue engineering. J Mater Sci Mater Med 22:405–416
11. Gurtner GC, Werner S, Barrandon Y et al (2008) Wound repair and regeneration. Nature 15:314–321
12. Harrison DE, Archer JR (1987) Genetic differences in effects of food restriction on aging in mice. J Nutr 117:376–382
13. Hubbard BP, Sinclair DA et al (2014) Small molecule SIRT1 activators for the treatment of aging and age-related diseases. Trends Pharmacol Sci 35:146–154
14. Hunt ND, Li GD, Zhu M et al (2012) Effect of calorie restriction and refeeding on skin wound healing in the rat. Age (Dordr) 34:1453–1458
15. Ikeda K, Torigoe T, Matsumoto Y et al (2013) Resveratrol inhibits fibrogenesis and induces apoptosis in keloid fibroblasts. Wound Repair Regen 21:616–623
16. Institute for Laboratory Animal Research (2011) Guide for the care, and use of laboratory animals. National Academies Press, Washington, DC
17. Jung SB, Kim CS, Kim YR et al (2013) Redox factor-1 activates endothelial SIRTUIN1 through reduction of conserved cysteine sulfhydryls in its deacetylase domain. PLoS One 8:e65415
18. Kasanen IH, Inhilä KJ, Vainio OM et al (2009) The diet board: welfare impacts of a novel method of dietary restriction in laboratory rats. Lab Anim 43:215–223
19. Kavalukas SL, Barbul A (2011) Nutrition and wound healing: an update. Plast Reconstr Surg 127:38S–43S
20. Klingberg F, Hinz B, White ES (2013) The myofibroblast matrix: implications for tissue repair and fibrosis. J Pathol 229:298–309
21. Kohen R, Nyska A (2002) Oxidation of biological systems: oxidative stress phenomena, antioxidants, redox reactions, and methods for their quantification. Toxicol Pathol 30:620–650
22. Maepa M, Razwinani M, Motaung S (2016) Effects of resveratrol on collagen type II protein in the superficial and middle zone chondrocytes of porcine articular cartilage. J Ethnopharmacol 3:25–33
23. Malfatti CR, Dos Santos FS, Wouk J et al (2017) Intracerebroventricular administration of the (1 → 6)-β-d-glucan (lasiodiplodan) in male rats prevents D-penicillamine-induced behavioral alterations and lipoperoxidation in the cortex. Pharm Biol 55:1289–1294

24. Ndiaye M, Philippe C, Mukhtar H et al (2011) The grape antioxidant resveratrol for skin disorders: promise, prospects, and challenges. Arch Biochem Biophys 15:164–170
25. Ni D, Xu P, Gallagher S (2016) Immunoblotting and immunodetection. Curr Protoc Immunol 114:8.10.1–8.10.36
26. Ohkawa H, Ohishi N, Yagi K (1979) Assay for lipid peroxides in animal tissues by thiobarbituric acid reaction. Anal Biochem 95:351–358
27. Ozaki M, Nakamura M, Teraoka S et al (1997) Ebselen, a novel anti-oxidant compound, protects the rat liver from ischemia–reperfusion injury. Transplant Int 10:96–102
28. Pearson KJ, Baur JA, Lewis KN et al (2008) Resveratrol delays age-related deterioration and mimics transcriptional aspects of dietary restriction without extending life span. Cell Metab 8:157–168
29. Polonini HC, Soldati PP, de Almeida PA et al (2015) Permeation profiles of resveratrol cream delivered through porcine vaginal mucosa: evaluation of different HPLC stationary phases. J Chromatogr B Anal Technol Biomed Life Sci 1002:8–12
30. Qiang L, Sample A, Liu H et al (2017) Epidermal SIRT1 regulates inflammation, cell migration, and wound healing. Sci Rep 26:14110
31. Reed MJ, Penn PE, Li Y et al Vernon RB, Johnson TS, Pendergrass WR, Sage EH, Abrass IB, Wolf NS (1996) Enhanced cell proliferation and biosynthesis mediate improved wound repair in refed, caloric-restricted mice. Mech Ageing Dev 31:21–43
32. Reiser K, McGee C, Rucker R et al (1995) Effects of aging and caloric restriction on extracellular matrix biosynthesis in a model of injury repair in rats. J Gerontol A Biol Sci Med Sci 50a:B40–B47
33. Rich L, Whittaker P (2005) Collagen and Picrosirius Red staining: a polarized light assessment of fibrillar hue and spatial distribution. J Morphol Sci 22:97–104
34. Roth GS, Kowatch MA, Hengemihle J et al (1997) Effect of age and caloric restriction on cutaneous wound closure in rats and monkeys. J Gerontol Biol Sci 52:B98–B102
35. Sell DR, Lane MA, Obrenovich ME et al (2003) The effect of caloric restriction on glycation and glycoxidation in skin collagen of nonhuman primates. J Gerontol A Biol Sci Med Sci 58:508–516
36. Simic P, Williams EO, Bell EL et al (2013) SIRT1 suppresses the epithelial-to-mesenchymal transition in cancer metastasis and organ fibrosis. Cell Rep 3:1175–1186
37. Smith JJ, Kenney RD, Gagne DJ (2009) Small molecule activators of SIRT1 replicate signaling pathways triggered by calorie restriction in vivo. BMC Syst Biol 3:31
38. Spanheimer R, Zlatev T, Umpierrez G et al (1991) Collagen production in fasted and food-restricted rats: response to duration and severity of food deprivation. J Nutr 121:518–524
39. Stankovic M, Mladenovic D, Ninkovic M et al (2013) Effects of caloric restriction on oxidative stress parameters. Gen Physiol Biophys 32:277–283
40. Sugino H, Hashimoto I, Tanaka Y (2014) Relation between the serum albumin level and nutrition supply in patients with pressure ulcers: retrospective study in an acute care setting. J Med Investig 61:15–21
41. Sung JS, Demple B (2006) Roles of base excision repair subpathways in correcting oxidized abasic sites in DNA. FEBS J 273:1620–1629
42. Thakur S, Dhiman M, Tell G (2015) A review on protein–protein interaction network of APE1/Ref-1 and its associated biological functions. Cell Biochem Funct 33:101–112
43. Todorovic V (2002) Food and wounds: nutritional factors in wound formation and healing. Br J Community Nurs 7:43–44, 46, 48
44. Vilhena MIM, Correa-Da-Silva MV, Arruda AC et al (2016) Measuring the antioxidant capacity induced by reduced thiols in human erythrocytes using SW-voltammetry. Int J Electrochem Sci 11:6453–6465
45. Xia J, Wu X, Yang Y et al (2012) SIRT1 deacetylates RFX5 and antagonizes repression of collagen type I (COL1A2) transcription in smooth muscle cells. Biochem Biophys Res Commun 428:264–270
46. Yaman I, Derici H, Kara C et al (2013) Effects of resveratrol on incisional wound healing in rats. Surg Today 43:1433–1438
47. Zeng G, Zhong F, Li J et al (2013) Resveratrol-mediated reduction of collagen by inhibiting proliferation and producing apoptosis in human hypertrophic scar fibroblasts. Biosci Biotechnol Biochem 77:2389–2396
48. Zhao P, Sui BD, Liu N et al (2017) Anti-aging pharmacology in cutaneous wound healing: effects of metformin, resveratrol, and rapamycin by local application. Aging Cell 16:1083–1093